IN THE UNITED STATES PATENT AND TRADEMARK OFFICE

Applicant:	Rehab Al-Jamal Naylor and David Harrison
Title:	"Tissue Repair by Modulation of Beta-1 Integrin Biological Function"
Appl. No.:	10/576,274
Filing Date:	10/18/2004
Examiner:	Maher M. Haddad
Art Unit:	1644
Confirmation Number:	9435

DECLARATION UNDER 37 C.F.R. § 1.132 OF REHAB AL-JAMAL

I, REHAB AL-JAMAL, do hereby declare:

1.   I obtained the degree of BSc (Hons) in Biomedical Sciences/Pharmacology and Toxicology (1993, Bradford University-UK) and PhD in the interaction between lung tissue mechanics, extracellular matrix proteoglycans and mechanical forces where the main focus was on lung tissue remodelling during injury (2001, Experimental Medicine/Meakins Christie Laboratories, McGill University-Canada). I have received training in pharmacology at SmithKline Beechams (1992). I have held a post-doctoral position (2001-2003) at Edinburgh University focusing on the role of integrins in cartilage mechanotransduction and how remodelling in osteoarthritis affects integrin function. Since 2003, I have held the position of co-principal investigator then principal investigator working on mechanisms of tissue injury, remodeling and repair. I have extensive experience in the field of tissue remodelling and repair as evident from an award for distinguished PhD student (McGill University, 2000) and continual project funding awarded by the Scottish Government (2 major project award 2003-2007

and 2008-2011) in addition to Edinburgh University departmental awards (2002-2003 and 2007-2008). I am the author and co-author of 5 major scientific publications which relate to the field of tissue remodelling and repair. I have given invited talks on the subject at Novartis (Horsham, UK) and the Swiss Federal Institute (Lausanne, Switzerland). In 2008, I was invited by the journal Pharmacology and Therapeutics to write a review detailing the role of beta1 integrin in tissue repair (Pharmacol Ther. 120(2):81-101.PMID: 18708090).

2.   I am one of the inventors on US Patent Application Serial No. 10/576,274.

FIRST EXPERIMENT

3.   Under my supervision, the JB1a antibody, which is known to modulate function of beta 1 integrin by binding to the beta 1 integrin molecule in a region of amino acid residues 82 to 87 comprising residues TAEKLK (SEQ ID NO:1) of the sequence of the mature beta 1 integrin molecule resulting in at least one of (i) an inhibition of the apoptotic pathway, (ii) an alteration in the metalloproteinase balance or (iii) an increase in the anabolism of the extracellular matrix, was administered after 6-hydroxydopamine (6-OHDA) induced dopaminergic injury in the substantia nigra in mice (mouse model for Parkinson's disease) using the following procedure:

3.1   Animals

Experiments were conducted using adult male C57/Bl6 mice (25-30 g; n=60). The animals were housed in cages (266mm x 425mm x 185mm. Floor area 800cm^2) in groups of five with free access to food (Standard Rat and Mouse No1) and water at a constant temperature of (21±1°C) with a normal 12 h light/dark cycle with lights on from 7:00 to 19:00. All surgical and behavioural procedures were conducted under the remit of a Project Licence in accordance with the UK Animals (Scientific Procedures) Act. Animals were used for experimentation between 9:30 am to 6:00pm.

3.2   Surgical Procedures

Surgery was performed under pentobarbitone anaesthesia (60mg/Kg, intraperitoneally) with the analgesic buprenorphine (Vetergesic®, 0.05 mg/kg, subcutaneous) being administered. Subsequently buprenorphine was administered post-

operatively as a jelly preparation placed in the recovery cages for voluntary use by the mice.

The anaesthetized animal was placed on a Kopf stereotaxic frame with a temperature-controlled mat. The incisor bar raised 1mm to ensure a level skull surface from the Bregma. An injection of saline (0.5ml, subcutaneous 0.9% sodium chloride, Baxter, U.K.) was given to replenish any loss of fluids. After shaving the head, the area was made sterile by applying microbiocidal aqueous iodine solution (Betadine; Seton, Healthcare, U.K.).

Using coordinates obtained from The Mouse Brain in Streotaxic Coordinates (K.B.J. Franklin and G. Paxinos eds., Academic Press, 1997) as a guide, preliminary experiments established the coordinates required for the unilateral intracerebral injections into the area of the substantia nigra in the right hemisphere. The coordinates were determined from Bregma: 3.5mm posterior, lateral 1.5 mm from the midline and 4.25mm vertical from the skull surface. A small incision (approximately 6mm) allowed retraction of the skin and create an entry through the skull using a burr drill. Following vehicle or drug injection, the hole was sealed using a dental acrylic cement.

Incisions were sutured using Ethicon sutures (5-0, Perma-Hand silk or coated Vicryl Plus, Johnson and Johnson). Post-surgery the antibiotic enrofloxacin (Baytril®, Bayer, 0.1% v/v) was administered in the drinking water. The animals were continuously monitored until recovery was achieved.

In some experiments, animals received a second intracerebral injection. Animals were again prepared as described and a skin incision was done avoiding the first incision site, and the very small dental acrylic skull sealant was removed and the second injection administered at the same coordinates. Incisions were sutured as above with the addition of Dermabond (Johnson and Johnson). Post-surgery the antibiotic enrofloxacin (Baytril®, Bayer, 0.1% v/v) was administered in the drinking water. The animals were continuously monitored until recovery was achieved.

Unilateral lesions were induced by the injection of vehicle (nitrogen bubbled normal saline) or 6-Hydroxydopamine (Sigma H116 6-Hydroxydopamine hydrobromide contains ascorbic acid as stabiliser). All injections were administered using a 5ul

Hamilton syringe and in a volume of 1ul volume injected over 5 minutes and the needle was left in position for a further 5 minutes.

The study plan is shown in Figure 1 of Appendix A. The anti-beta 1 integrin antibody, JB1a (J.A. Wilkins, Manitoba) was dialysed against diluted phosphate buffered saline, lyophilised and reconstituted so as to obtain a concentration of 50ug/ul. 6-Hydroxydopamine was dissolved in nitrogen-bubbled saline at 1 or 2 ug/ul for the dose-effect study and 2ug/ul for the post-treatment groups.

Due to the sensitivity of 6-hydroxydopamine to neutral pH and in a preliminary experiment, the administration of the anti-beta 1 integrin antibody with 6-hydroxydopamine simultaneously was precluded

3.3   Behavioural observations

Experiments were carried out in a sound proofed, diffusely illuminated room maintained at a temperature of 21 ± 1 °C.

3.4   Assessment 1

In the first analysis, animals were placed into an observation cage of the same dimensions as the holding cages. Animals received no drug treatment and the direction of their movement within the cage was monitored and the nature of the motor behaviour assessed and recorded by the observer and verified by a second present observer. The direction of movement was characteristically around the edge of the cage with forays across the cage. Movements of the mouse to the side opposite the hemisphere of injection was considered "Left"(L) directed movement; movement to the same side of injection was considered "Right" (R) directed movement. Traversing a side of the observation cage was recoded as one movement. Also, an animal that exhibited a tight pivotal movement on its axis was also scored as one movement. Preliminary studies established that a 5-minute observation period was adequate to reliably score the animal for right and left movements.

3.5   Assessment 2

Animals were administered the dopamine receptor agonist, apomorphine 0.5mg/kg subcutaneously ((S)-(+)-Apomorphine hydrochloride hydrate, D043 Sigma-Aldrich, Stock solution of 0.1 mg/ml in 0.9% w/v saline and 0.1% w/v sodium metabisulphite) and placed in the observation box. Apomorphine is well established to

induce a circling response in rodents via an action on dopamine receptors, the direction of movement, left or right, as described in Assessment 1, reflecting drug action on receptors of enhanced sensitivity. Observation was carried out for 30 to assess the direction of movement.

After the assessments, animals were terminated by overdose of pentobarbitone and the brains removed quickly and fixed in 10% w/v neutral buffered formalin for 24 hours and then paraffin-embedded. Serial sections of the substantia nigra were cut at 3um; two of which stained with Haematoxylin and Eosin. The remaining sections were using for immunofluorescence staining.

3.6   Statistical analysis

Over all effects of 6-OHDA, vehicle and antibody treatment on circling behaviour were estimated using multivariate ANOVA. Post-hoc comparisons were made using Tukey's test. P values less than 0.05 were considered statistically significant.

RESULTS

4.   Results are shown in Figures 2 to 11 of Appendix A as follows:

Figure 2. Circling behaviour without apomorphine: effect of vehicle volume;

Figure 3. Circling behaviour without apomorphine: effect of 6-OHDA dose;

Figure 4. Circling behaviour without apomorphine: effect of 3 days post-treatment with the anti-beta1 integrin antibody, JB1a, on 6-OHDA-induced circling;

Figure 5. Circling behaviour without apomorphine: effect of 7 days post-treatment with the anti-beta1 integrin antibody, JB1a, on 6-OHDA-induced circling;

Figure 6. Circling behaviour with apomorphine: effect of vehicle volume;

Figure 7. Circling behaviour with apomorphine: effect of 6-OHDA dose;

Figure 8. Circling behaviour with apomorphine: effect of 3 days post-treatment with the anti-beta1 integrin antibody, JB1a, on 6-OHDA-induced circling; and

Figure 9. Circling behaviour with apomorphine: effect of 7 days post-treatment with the anti-beta1 integrin antibody, JB1a, on 6-OHDA-induced circling.

The assessment of spontaneous mouse movement to the right or left provides a simple model to detect overt motor impairment. The neurotoxic action of 6-OHDA has been used for over 25 years as a model of Parkinson's disease. The study revealed that spontaneous movements of mice in an observation cage following the injection of vehicle at different volumes as a unilateral injection into the substantia nigra was not statistically significant (Figure 2). The injection of 6-OHDA into the substantia nigra induced spontaneous movements to the left which was dose-dependent (Figure 3). Administration of JB1a into the substantia nigra 3 days after the injection of 6-OHDA showed no significant effect on spontaneous movement between vehicle (saline), JB1a or 6-OHDA from non-treated (sham) animals (Figure 4). However, when administered 7 days after 6-OHDA, JB1a inhibited movement abnormality by significantly reducing the left directed movements by some 50 per cent (Figure 5).

Following the subcutaneous administration of apomorphine to mice that had received a unilateral injection of vehicle, JB1a or 6-OHDA into the substantia nigra in the right hemisphere, circling movements to the right were generally increased by 40/50 per cent as compared to sham treated controls. The study revealed that circling movements of mice in an observation cage following the injection of vehicle at different volumes as a unilateral injection into the substantia nigra was statistically significant (Figure 6). The injection of 6-OHDA into the substantia nigra induced circling movements to the left which was dose-dependent (Figure 7). Administration of JB1a into the substantia nigra 3 days after the injection of 6-OHDA showed no significant effect on circling movement between JB1a or 6-OHDA animals (Figure 8). However, when administered 7 days after 6-OHDA, JB1a significantly reduced the circling movements by some 50 per cent (Figure 9); the values returning to those observed in the sham operated group.

Circling behaviour is revealed by a unilateral lesion of the dopaminergic system, followed by a provocative challenge with a dopamine receptor agonist, e.g. apomorphine. Normally, it is hypothesised that the ascending nigrostriatal pathways in the two hemispheres act in unison to regulate normal motor behaviour. A modest decrease in normal dopamine function in one hemisphere will be balanced by a reduced function in the other. In the present animal model this explains the apparent normality of spontaneous motor behaviour. The mice can move forward and to the left or right at will.

However, following denervation, the dopamine receptors in the denervated hemisphere (within the striatal complex) develop hypersensitivity to dopamine agonist challenge, driving the animals in the opposite direction (i.e. in the above experiments to the left.

CONCLUSION OF FIRST EXPERIMENT

5.   Based on the data presented in Appendix A, I conclude that JB1a promoted tissue repair in a mouse model of Parkinson's disease.

SECOND EXPERIMENT

6.   Under my supervision, the pharmacological mode of action of JB1a-mediated effect on beta1 integrin was investigated as follows:

6.1   Downstream signalling phosphoprotein activity measurements using human mesenchymal and epithelial cell co-culture in vitro

Adult human lung fibroblasts (CCD-8Lu) were seeded onto collagen I coated BioFlex 6 well plates at 0.5 X 106/well. The following day, NCI-H441 were seeded on top of the fibroblasts at the same density. NCI-H441 cells possess alveolar type II cell characteristics. Cells were starved with media containing 0.1% FCS. The plates were subjected to stretching at 2-10% sinusoidal stretch at 1Hz for 0.5, 1 or 3 hours. PPE was added at 0.3U/ml alone or in combination with JB1a (2µg/ml) or K20 (1µg/ml). At the end of the treatment period, the media was aspirated and total protein lysates were obtained using the Multiplex lysis buffer (BioRad) according to the manufacturers' instructions. 15-multiplex phosphoprotein kit was used for measurement of selected phosphoproteins according to the manufacturers' instructions (BioRAD).

6.2   Three-dimensional confocal microscopy
In a separate set of experiments lung fibroblasts and epithelial cells were seeded onto collagen I coated glass coverslips MatTek dishes as described above. The cells were starved in media containing 0.1% FCS then exposed to the same conditions as described above.

At the end of the treatment period the media was removed and cells were fixed using 4% paraformaldehyde for 5 minutes. After rinsing with PBS, the coverslips were

subjected to double immunofluorescence staining for beta1 integrin. The first labelling was done after blocking with Universal Block (dako) using the ligand-competent conformation recognising antibody, 9EG7 followed by Alexa 488 labelled anti-rat IgG antibody. The coverslips were then blocked using Power Block and then probes using K20 antibody followed by Alexa-548 labelled anti-mouse IgG. The The nuclei were visualised using TO-PRO3. Images were collected through 3 separate channels (9EG7 488: $\lambda = 488$, K20 $\lambda = 548$, nuclei: $\lambda = 647$ nm) using x63 oil lens and Zeiss LSM510 CLSM inverted microscope. The resulting images were analysed with Imaris software (Bitplane AG, Switzerland). Three-dimensional images were reconstructed.

6.3   Beta1 integrin extraction and analyses

NCI-H441 cells and human lung fibroblasts were cultured as described above. Media was changed prior to the experiment to 0.1% FCS containing media. Vehicle, PPE (0.3U/ml) or PPE in the presence of JB1a (1µg/ml) containing media was added onto the cells for 1 or 2 hours. Cells were extracted using MEM-ER lysis buffer (Pierce) to isolate membrane and soluble fractions according to manufactures'' instruction.

The membrane fractions were subjected to dialysis against tris-buffered saline overnight at 4oC using microdialysis cassettes (Pierce). Total protein was quantified using Lowry method (Sigma). Fractions were separated (20ug/well of membrane fractions and 40ug/well of soluble fractions) onto 10% SDS-PAGE and transferred onto nitrocellulose membranes then probed for beta1 integrin using JB1a and developed with HRP-conjugated secondary antibodies using the ECL-plus chemiluminescence system (Amersham Biosciences).

6.4   Probes for FRET

Octadecyl rhodamine B chloride (R18) was from Molecular Probes. The VLA4 specific peptide derivative 4-((n9-2-methylphenyl)ureido)-phenylacetyl-L-leucyl-L-aspartyl-L-valyl-L-prolyl-L-alanyl-L-alanyl-L-lysine (LDV peptide derivative) and its FITC-conjugated analogue were synthesised at Commonwealth Biotechnologies (Richmond, VA).

6.5   Flow cytometry

All fluorescence measurements were performed on a Becton-Dickinson FACScan flow cytometer interfaced to a Macintosh using the CellQuest software package. The

FACScan is equipped with an argon ion laser with output fixed at 488 nm. The acquisition was conducted at low flow rate so as to achieve 400-500 events/second.

6.6 Equilibrium binding of LDV-FITC to alpha4beta1-integrins on Jurkat cells

Jurkat cells (ATCC) were suspended at ~ 10^6 cells/ml and were treated with a range of concentrations of the fluorescent ligand (typically 0–8 nM) in the presence of divalent cations (0.5-3 mM Mn^{2+}, 0.5-1 mM Mn^{2+}+ 1 mM Ca^{2+}, and 1 mM Ca^{2+}). Nonspecific binding was determined using 500-fold excess unlabeled peptide. All experiments were performed in Hanks buffered salt solution (Invitrogen) containing 0.1% FBS.

6.7 Kinetic FRET analysis of binding in Jurkat cells

Kinetic analysis was done as described previously (Chigaev et al., 2001,2003). Briefly, cells (10^6 cells/ml) were analysed for 30–120 s to establish a baseline, then the fluorescent ligand LDV-FITC was added, and FACS acquisition was immediately re-established, losing 5–10 s of the total time course. Next, samples were incubated with different concentrations of R18 (up to 10 uM) for 1 min. Donor intensities (FL1) were measured using a BD Biosciences FACScan flow cytometer as described above. The quenching curves generated using the following procedure characterise the distance of closest approach between the integrin head group and the surface lipid membrane as an index of change integrin conformation. The resulting data were converted to mean channel fluorescence over time using FLOWJO software.

6.8 FRET Detection of Integrin Conformational Activation

For real-time antibody-induced conformational classification experiments, Jurkat cells were preincubated with 4 nM LDV-FITC-containing small molecule for 1 min. Then, data were acquired for 30–120 s to establish a base line, and various antibodies were added. Acquisition was re-established, and data were acquired continuously for up to 60 s before adding 5uM R18 and recommencing the acquisition. Donor intensities (FL1) were measured using a BD Biosciences FACScan flow cytometer. The quenching curves generated using the following procedure characterize the distance of closest approach between the integrin head group and the surface lipid membrane as was shown previously. The resulting data were converted to mean channel fluorescence over time using FLOWJO software.

6.9   Statistical Analysis

Curve fits and statistics were determined using GraphPad Prism and SPSS. Mean values are presented. Each experiment was repeated three times.

RESULTS

7.   Results are shown in Figures 1 to 9 of Appendix B as follows:

Figure 1 shows the effect of JB1a on elastase-induced changes on a) the levels of signalling phosphoproteins (p-AKT, p-cJUN and p-JNK), b) ligand competency as shown in images showing the effect of vehicle, elastase and JB1a on 9EG7 staining *in vitro* using human lung co-culture, c) beta1 integrin cellular localisation;

Figure 2 shows the effects of K20 and AIIB2 anti beta1 integrin antibodies on elastase-induced changes on a) the levels of signalling phosphor-proteins (p-AKT, p-cJUN and p-JNK), b) ligand competency as shown in images showing the effect of vehicle, elastase and JB1a on 9EG7 staining *in vitro* using human lung co-culture, c) beta1 integrin cellular localisation.;

Figure 3 shows theoretical 3D reconstruction of extracellular domain of beta1 integrin and the site of binding for JB1a;

Figure 4 shows the dose-response binding curves for LDV-FITC in Jurkat cells;

Figure 5 shows the dose-response of FRET efficiency using 4nM LDV-FITC and varying concentrations of R18;

Figure 6 shows the effect of varying doses of JB1a on LDV-FITC fluorescence emission and LDV/R18 pair FRET efficiency;

Figure 7 show the dose of JB1a were stable FRET was achieved;

Figure 8 shows a) the protocol of addition of various treatments, b) fluorescence of LDV-FITC over time before and after the additions of various antibodies against beta1 integrin and R18 under basal conditions, and c) differences in the quenching curves of the various treatments; and

Figure 9 shows a summary of FRET efficiencies of LDV-FITC/R18 pair in the presence of various antibodies under basal and activated conditions (using 0.5mM Mn^{2+}).

Upon activation, integrin-linked kinase (ILK) binds to the cytoplasmic domain of the beta1 integrin subunit. In turn, ILK activates multiple signalling pathways such as protein kinase B (PKB/AKT) and inhibits glycogen synthase kinase-3beta (GSK-3beta) activity affecting transcription factor binding to their DNA sequences. This effect is, in part, through phosphorylation which reduce transcription factor binding to their DNA sequences such as AP-1 and CREB activity. As a model of tissue remodelling in disease, we investigated the activity of beta1 integrin in an in vitro elastase injury system. A co-culture of primary, adult human lung fibroblasts was overlayered with NCI-H441 lung cells, under cyclic mechanical stimulation, and subjected to elastase treatment.

To investigate the involvement of beta1 integrin activation in elastase-induced signalling changes, we used three different monoclonal antibodies against beta1 integrin. We targeted the beta A and the hybrid domains, both of which are implicated in the control of integrin conformational changes. The first is the adhesion blocking clone JB1a which targets primarily the amino acids 82-87 comprising part of the hybrid domain. We also used the adhesion blocking clone AIIB2, which binds amino acid residues 207-218 within the A-domain, and the K20 clone, widely reported to have no functional effects which binds the hybrid/EGF repeat region.

Addition of elastase to cell culture induced an increased phosphorylation of signalling proteins known to act downstream of beta1 integrin (Figure 1a). During the course of injury pAKT levels increased followed by transient increases in phospho-cJUN and phospho-JNK (Figure 1a).

When beta1 integrin was bound by antibody clone JB1a in the no injury control group there was no significant effect on downstream beta1 integrin MAPK and AKT signalling pathways. However, in a setting of injury JB1a inhibited all elastase-induced changes in phosphorylation of the measured signalling proteins. This effect was not seen with either AIIB2 or K20. (Figure 2a). Therefore, targeting the hybrid domain using JB1A inhibits elastase induced beta1 integrin activation.

Alteration in conformation can occur with affecting receptor binding activity. We examined the effects of elastase on ligand binding activity of beta1 integrin using the ligand competent specific anti-beta1 integrin antibody 9EG7. Elastase caused an increase in ligand competent/active beta1 integrin expression in addition to enhancing its

clustering. Inhibition of beta1 integrin, using JB1a alone, appeared to increase the level of ligand-competent beta1 integrin but inhibited elastase-induced clustering (Figure 1b). The anti-beta1 integrin clone K20 induced clustering of beta1 integrin together with an increase in the ligand-competent conformation (Figure 2b); an effect previously noted.

The effects of elastase and JB1a on the level of ligand-competent receptor were not simply as a result of change in cell surface expression (Figure 1c). However, elastase increased the cytosolic fraction-associated beta1 integrin, which could be attributed to recycling or degradation (Figure 1c). The non-functional clone K20 increased membrane associated beta1 integrin (Figure 2c).

The separation of the alpha and beta subunit legs is a critical step in integrin activation to transform the bent structure to an extended conformation, thus allowing headpiece-ligand engagement. Therefore we questioned whether the effect seen with JB1a is due to its effect on beta1 integrin chain allostery. Indeed, targeting amino acid sequences within the hybrid domain region using antibodies has been reported to stabilise the physiological intermediate state of the receptor in a similar fashion as an allosteric antagonist (Figure 3).

To address this question we conducted FRET studies using the non adherent Jurkat cells which express alpha4beta1 integrin. FITC labelled LDV cyclic peptide was used to label the head of alpha4beta1 integrin and the lipophillic dye R18 was used to label the cell membrane. LDV-FITC acts as a donor and R18 as an acceptor. FACS was used for the FRET acquisition and measurements.

The concentration for LDV-FITC was chosen on the basis of saturable binding as demonstrated in Figure 4 to be 4nM. The concentration of R18 selected was selected on the basis of maximal FRET efficiency without causing detrimental effects to the cells as shown in Figure 5. The maximum concentration were FRET plateau was achieved was 5uM. At 10uM concentration the cells exhibited necrotic cell death.

Various concentrations of JB1a were used to ascertain stable FRET effect and saturable binding without interfering with the FRET pair (Figures 6 and 7).

When compared to other anti-beta1 integrin functional clones, JB1a exhibited FRET efficiency indicative of an intermediate partially extended conformation when

compared to Mn^{2+}-induced conformation activation and other known inhibitory or activating antibodies (Figures 8 and 9).
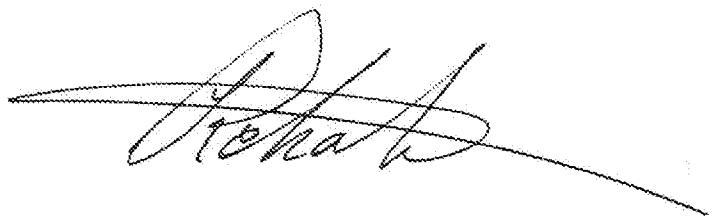
CONCLUSION OF SECOND EXPERIMENT

8.   Based on the data presented in Appendix B, I conclude that the pharmacological mode of action of JB1a-mediated effect on beta1 integrin is as an allosteric dual agonist/antagonist. The functional modulation is a unique pharmacological mode of action which was not described before. JB1a acts as agonist/antagonist which is demonstrated by its effect on downstream signaling with and without injury and its conformation effect from the FRET. The FRET experiments show clearly that JB1a, unlike all its previously described inhibitory counterparts, can have an effect resembling that of some previously described activating anti-beta1 integrin clones.

9.   Our work has also demonstrated efficacy of modulating beta1 integrin in **arthritis** both *in vitro* (using IL1 beta-induced chondrocytes injury) and *in vivo* (in mouse model of adjuvant–induced monoarthritis). The *in vivo* model testing was done by administering the antibody after the induction of arthritis. Additionally, we have *in vitro* data on beta amyloid-induced primary human cortical neuronal injury. This model exemplifies some feature of **Alzheimer's**.

10.   I further declare that all statements made herein of my own knowledge are true and that all statements made on information and belief are believed to be true, and further, that these statements were made with the knowledge that willful false statements and the like so made are punishable by fine or imprisonment, or both, under Section 1001 of Title 18 of the United States Code, and that such willful false statements may jeopardize the validity of the application or any patent issuing thereon.

Signed this __15th__ day of __December____, 2009.

REHAB AL-JAMAL, Ph. D.